galaxies

MDPI

Review

The Seeding of Cosmic Ray Electrons by Cluster Radio Galaxies: A Review

Franco Vazza [1,2,3,*] and Andrea Botteon [2]

[1] Dipartimento di Fisica e Astronomia, Universitá di Bologna, Via Gobetti 93/2, 40129 Bologna, Italy
[2] INAF-Istituto di Radio Astronomia, Via Gobetti 101, 40129 Bologna, Italy; andrea.botteon@inaf.it
[3] Hamburger Sternwarte, Universität Hamburg, Gojenbergsweg 112, 41029 Hamburg, Germany
* Correspondence: franco.vazza2@unibo.it

Abstract: Radio galaxies in clusters of galaxies are a prominent reservoir of magnetic fields and of non-thermal particles, which become mixed with the intracluster medium. We review the observational and theoretical knowledge of the role of these crucial ingredients for the formation of diffuse radio emission in clusters (radio halos, relics, mini halos) and outline the open questions in this field.

Keywords: AGN feedback; radio jets; galaxy evolution; clusters of galaxies

Citation: Vazza, F.; Botteon, A. The Seeding of Cosmic Ray Electrons by Cluster Radio Galaxies: A Review. *Galaxies* **2024**, *12*, 19. https://doi.org/10.3390/galaxies12020019

Academic Editor: Fulai Guo

Received: 25 March 2024
Revised: 15 April 2024
Accepted: 17 April 2024
Published: 22 April 2024

1. Introduction

Jets from radio galaxies can store the majority of their internal energy in the form of non-thermal components (relativistic particles and magnetic fields), although the balance between thermal and non-thermal components may depend on the radio galaxy type, as well as on the interaction with the surrounding environment, e.g., [1,2]. Given the very active dynamics of the intracluster medium (ICM) under the effect of the episodic accretion of gas and dark matter, e.g., [3–7], as well as of the powerful feedback from radio galaxies themselves, e.g., [8–12], it appears unavoidable that such interactions result in the fueling of a prominent and potentially visible reservoir of magnetic fields and non-thermal particles in the ICM, e.g., [13,14].

Recent deep radio observations have detected complex morphologies of remnant plasma, injected by radio galaxies and in different stages of mixing with the surrounding environment, e.g., [15–19], and often in conjunction with diffuse ∼Mpc-sized cluster radio sources.

In the case of "radio relics" (i.e., elongated and polarized radio sources that are typically co-located with merger shock waves; see, e.g., [20] for a review), a pre-existing population of low-energy relativistic electrons is often required to explain the brightness of radio relics associated with weak $\mathcal{M} \leq 2.5$ shocks, in which case shock re-acceleration, rather than the injection of freshly accelerated electrons from the thermal pool, can be hypothesized, e.g., [21–24]. In "radio halos" (i.e., centrally located, roughly spherically symmetric and unpolarized sources believed to trace turbulence in clusters with recent mergers; see, e.g., [25] for a review), fossil electrons are required to allow Fermi II turbulent re-acceleration to produce the observed level of radio emission, which also shows hints of curvature at high energies. Similar requirements have been proposed to explain "radio mini-halos" (smaller than radio halos and preferentially found in cool-core clusters, e.g., [26,27]) and also the pervasive emission recently detected at the extreme periphery of clusters and in between pairs of interacting clusters of galaxies, e.g., [28–36].

In this review, we wish to present the state of the art of the existing observational evidences for the mixing of plasma ejected by radio galaxies with the ICM (Section 2), and to give the status of our theoretical and numerical understanding of this process, which requires the understanding of the dynamics of the ICM across a wide range of spatial scales (Section 3).

2. Observations

The electrons emitted in diffuse cluster radio sources are, in most cases, expected not to be accelerated in situ. Radio phoenixes and disturbed radio tails, such as those shown in Figure 1, represent the clearest evidence of how the relativistic plasma ejected by cluster AGN can seed the ICM with non-thermal components while being mixed and distributed in the surrounding environment by thermal gas motions.

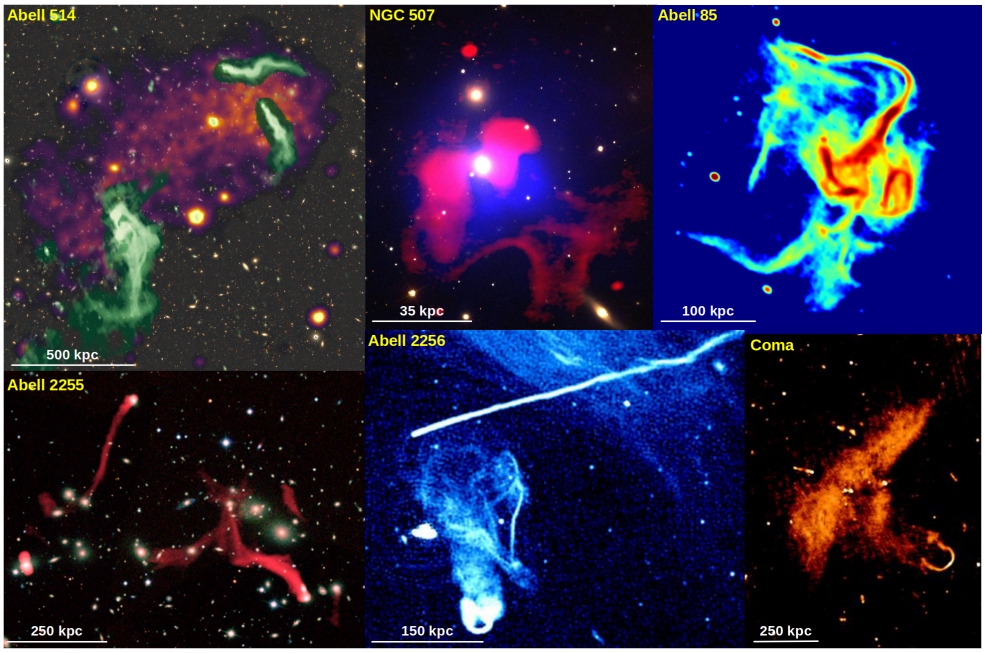

Figure 1. Examples of ongoing cosmic ray seeding and interaction between radio galaxies and thermal gas. From top left to bottom right: AGN with bent radio tails (green) due to the interaction with the X-ray gas (purple) in Abell 514 [37]; radio plasma (red) transported by thermal gas (blue) sloshing motions in the NGC 507 group [19]; the filamentary radio phoenix in Abell 85 [38]; the complex system of filamentary-tailed radio AGN (red) at the center of Abell 2255 [39]; the radio phoenix and the long head–tail radio galaxy in Abell 2256 [40]; and a radio galaxy feeding the radio relic in the Coma cluster [41].

2.1. Radio Phoenixes

Radio phoenixes are diffuse radio sources with sizes of a few hundred kpc at most, characterized by ultra-steep spectra ($\alpha > 1.8$, where $I(\nu) \propto \nu^{-\alpha}$ is the radio emission spectrum) showing high-frequency spectral steepening. They trace fossil radio plasma ejected from past episodes of AGN activity (also called "AGN remnants"), revived by the dynamical motions within the ICM. Consequently, such types of emission are also referred to as "revived fossil plasma". As a result of interactions with the thermal gas, phoenixes typically show amorphous morphologies, with an often unclear connection with the host galaxy that originally ejected the radio plasma (cf., Figure 1).

Despite radio phoenixes (before the term "phoenix" was introduced in Ref. [42] these sources were called "relics"; nowadays, the term "radio relic" is used to classify large and arc-shaped diffuse emission associated with shock fronts in cluster outskirts) have been known for about three decades, e.g., [43–47], with the advent of high-quality observations, and particularly at $\lesssim$1 GHz frequencies (where the radio emission appears brighter due to its steep spectral index), in recent years the number of these sources has significantly increased, e.g., [17,39,48–55]. Instances of phoenixes with extreme spectral indexes of >2.5 have also been found, e.g., [45–47,50,56]. High-resolution images have started to reveal their complex morphologies, often characterized by filamentary structures [17,38,57–59]; see, for example, the remarkable cases of the phoenixes in Abell 85 and Abell 2256 reported in Figure 1. The existence of these phoenixes indicates the presence of extended patches of

old, relativistic electrons in the sub-GeV energy range in the ICM. Although these electrons are fully relativistic (their Lorentz factor is $\gamma \sim 100$), they are usually considered as low-energy or even "mildly relativistic" electrons in this context, considering that the electrons emitting detectable radio emission have a $\geq$GeV energy (corresponding to $\gamma \gg 10^3$). While statistical studies on the properties of radio phoenixes, such as their occurrence with cluster mass and dynamical state, are still lacking, the recent observations of large samples of clusters, e.g., [60–66] suggest that sources of fossil plasma may be very common, if not ubiquitous, in all clusters of galaxies, especially at lower frequencies.

2.2. Disturbed Radio Tails

Jets originating from supermassive black holes residing in cluster AGN are deflected by the ram pressure while their host galaxy moves through the ICM ($P_{\rm ram} \propto \rho v^2$, where ρ is the ICM density and v is the relative velocity between jets, or the galaxy, and the ICM), generating the so-called tailed radio sources [67]. Depending on the degree of jet bending, these sources can be classified as wide-angle tails (WATs), narrow-angle tails (NATs), or head–tails (HTs). The most spectacular tailed radio galaxies can extend beyond the Mpc scale, leaving a long trail of non-thermal plasma behind their path through the ICM. This material is eventually dispersed in the environment. Relativistic electrons in the magnetized ICM primarily lose their energy via synchrotron and inverse Compton losses on the short timescale given by $t_{\rm cool} \sim \gamma/\dot{\gamma} \sim 10$ Myr (using $\gamma = 10^4$, $B = 1$ μG and $z = 0$ as reference values for the ICM), e.g., [68]. The cooling timescale approximately scales inversely with the energy of the electrons ($t_{\rm cool} \propto 1/\gamma$); hence, the least energetic electrons in tails are found at larger distances from the AGN, and steeper synchrotron spectra are progressively found along the tail. As a result, radio tails appear longer at lower frequencies.

However, new highly sensitive radio observations (again, mainly at low frequency) are revealing that tails (i) often exhibit longer extensions than expected from the radiative lifetime of relativistic electrons, e.g., [69]; (ii) may feature regions of surface brightness and spectral index flattening (contrary to the gradual steepening expected by particle aging) [15,70,71]; and (iii) frequently display disturbed morphology, especially at their terminal ends, where the tail structure "breaks", e.g., [16,49,60,72–76]; see Figure 1. These properties suggest a non-trivial ongoing interplay between the non-thermal components in tails and the surrounding thermal gas, leading to processes that can sustain particle lifetimes for periods of time and distances longer than usually expected. Radio tails, thus, naturally fuel the cluster environment with seed mildly relativistic electrons, and the latter can be re-energized in this first interaction with the ICM, i.e., even before they are re-accelerated again by the processes leading to diffuse radio emissions (see next section).

2.3. Evidence of Interaction with the ICM and Connection with Large-Scale Diffuse Radio Emission

Shock, cold fronts, turbulence, and sloshing in the ICM can significantly influence the fate and morphology of non-thermal plasma ejected by cluster radio galaxies. Nowadays, radio and X-ray observations are providing clear evidence of this kind of interaction in many clusters (Figure 1). Shocks or cold fronts co-located with sudden direction changes of radio galaxy tails have been reported in Abell 3411 [77], Coma [78], Abell 3376 [79], Abell 1775 [49], Abell 3562 [80], Abell 514 [37], and are invoked in other cases to explain the disturbed morphology of the radio emission [81–84]. Shocks can re-energize cosmic ray electrons both via re-acceleration (Fermi I processes) and adiabatic compression, e.g., [85–87]. Shear flows inside cold fronts stretch and amplify magnetic fields, e.g., [79,88], possibly dragging the relativistic plasma with them in tangential directions, e.g., [19,37,79,80,84,89]. Turbulence, either induced by cluster–cluster mergers or by sloshing or by the wake of a fast-moving radio galaxy, can trigger Fermi II re-acceleration mechanisms [90–94]. In the extreme case of the so-called "gently re-energized tail" (GReET) in Abell 1033, a turbulent re-acceleration mechanism acting on a timescale comparable to that of relativistic electrons, barely balancing their cooling, has been proposed to explain the observed radio proper-

ties [15,71]. Adiabatic compression of fossil plasma due to a recent shock passage is also the favored formation scenario for radio phoenixes [85]. However, as of now, the detection of a shock front at the location of a radio phoenix has been reported only in Abell 2443 [95], leaving the formation scenario for these sources still uncertain (although the detection of shock-heated gas co-located with phoenixes has also been claimed in some cases [96–99]).

Evidence of the seeding of radio halos and relics by radio galaxies has also been reported. Radio galaxies embedded into radio relics suggest the ongoing seeding of cosmic ray electrons in the environment [41,77,100–104]. In the case of Abell 3411, a clear connection between a radio galaxy compressed by a shock front and a radio relic has been used to support the scenario in which particles are re-accelerated by the weak shock [77], and to test the adiabatic compression scenario [105]. Radio galaxies whose tails fade into radio halos or that demonstrate a complex mixing with central non-thermal diffuse emission/turbulent motions have been also associated with the seeding of cosmic rays on cluster scales, e.g., [16,30,32,39,54,84,106]. Recently, a connection between a radio phoenix and central diffuse emission in Abell 85 has also been reported [107].

Although here we focus on systems with strong indications of interaction between AGN radio plasma and diffuse radio emission on larger scales, it is worth noting that several interesting observations have detected different stages of the likely interplay between radio galaxies and the surrounding medium, e.g., [108–112], to cite a few. These interactions are often characterized by filamentary radio structures, which can, in principle, yield precious information about the life cycle of relativistic fossil electrons in the ICM.

Despite the observational evidence of the seeding of cosmic ray electrons by cluster radio galaxies, a number of questions still need to be addressed. What is the contribution of the single dynamical processes (shocks and turbulence) in the redistribution and re-acceleration of cosmic ray electrons in clusters? How many radio galaxies are needed to fuel the ICM with non-thermal particles? Is a direct connection between radio galaxies and diffuse sources always needed to explain the emission from radio halos and relics? What about diffuse sources that do not show such a connection with cluster AGN?

3. Theoretical and Numerical Models

One of the very first seminal works on this subject [113] noted that the contribution from a few radio galaxies hosted in the Coma cluster may explain the normalization of the observed radio halo emission, provided that the magnetic field in the entire region was of order $\sim \mu G$. Similar estimates were later attempted for different systems, e.g., in A3562 [114], or more recently for A2163 [31], just to cite a few.

A rough estimate can be obtained assuming energy equipartition between the relativistic electrons—also including those not emitting at the frequency of radio observations—the ICM magnetic field, and possibly the additional cosmic ray protons in the system (whose energy ratio with respect to electrons is K), assuming a power-law distribution of cosmic ray electrons between $\gamma_{\rm min}$ and $\gamma_{\rm max}$ ($N(\gamma) = N_0 \gamma^{-\delta}$). Here, we follow the formalism in [115], where the equipartition magnetic field, $B_{\rm eq}$, was computed, also considering the contribution from cosmic ray electrons with energies below the observing frequencies as

$$B_{\rm eq} = [C(\alpha) \frac{P(\nu)\nu^{\alpha}}{\phi V}(1+K)]^{\frac{1}{\alpha+3}} \gamma_{\rm min}^{\frac{1-2\alpha}{\alpha+3}} \quad (1)$$

where $P(\nu)$ is the radio emission (in units erg/s/Hz), ν is the observing frequency (in Hz), $\alpha = (\delta - 1)/2$ is the radio spectral index, V is the volume of the emitting region (in cm^3), and ϕ is the filling factor. $C(\alpha)$ is a function of the spectral index, whose expression is given by Equation (A3) in [115]. The total energy of cosmic ray electrons (in units of erg) across their entire energy range is thus given by

$$U_{\rm CRe} = \frac{2\phi V}{\alpha + 1} \frac{B_{\rm eq}^2}{(1+K)8\pi} = m_e c^2 N_0 \int_{\gamma_{\rm min}}^{\gamma_{\rm max}} \gamma^{-\delta+1} d\gamma \quad (2)$$

From the above relation, we derive the total number of electrons, which has the advantage of being a conserved quantity within the cluster volume (regardless of radiative losses or re-acceleration by turbulence). It should be noted that the above estimate neglects the possibility of a continuous production of secondary electrons by the hadronic process [116], which, however, cannot be the dominant process to explain radio halos given the very tight constraints imposed by the non-detection of hadronic γ-ray emission by high-energy observations, e.g., [117–119].

The total number of cosmic ray electrons can thus be computed with

$$N_{\rm CRe} = \frac{U_{\rm CRe}}{m_e c^2} \cdot \left(\frac{-\delta + 2}{-\delta + 1} \right) \cdot \left(\frac{\gamma_{\rm min}^{-\delta+1} - \gamma_{\rm max}^{-\delta+1}}{\gamma_{\rm min}^{-\delta+2} - \gamma_{\rm max}^{-\delta+2}} \right). \quad (3)$$

One can use the above relation, after specifying the minimum and maximum energies of the cosmic ray electron population, to estimate the number of electrons required by an observed radio structure for which energy equipartition can be reasonably hypothesized.

The left panel of Figure 2 gives the total number of cosmic ray electrons under different model variations (e.g., for different values of K, $\gamma_{\rm min}$) for a radio halo with volume $V = 1^3$ Mpc^3 at $z = 0$ and with a typical radio power of 10^{32} erg/s/Hz at 144 MHz, for different values of the radio spectral index. The right panel of the same figure shows the number of electrons as a function of the radio power instead, by fixing the spectrum to a reference value of $\alpha = 1.3$.

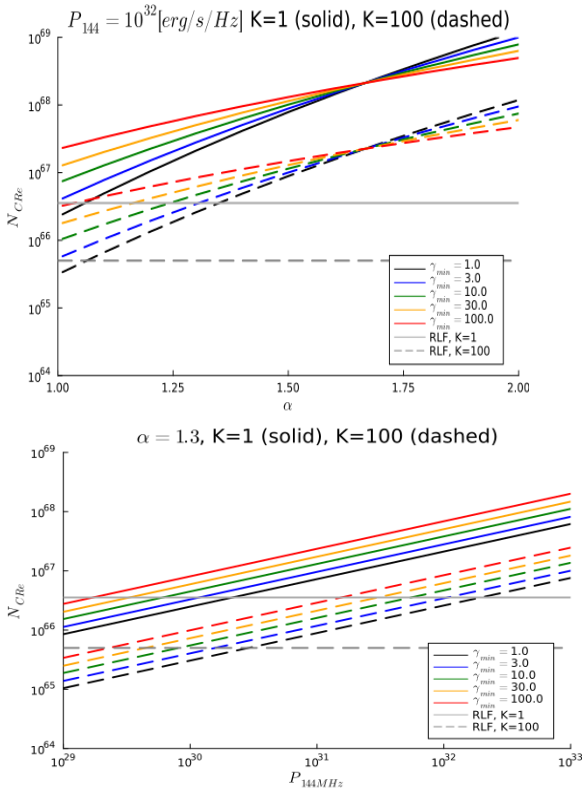

Figure 2. Top panel: Number of cosmic ray electrons to explain a radio halo emitting 10^{32} erg/s/Hz at 144 MHz, as a function of the observed radio spectrum (α) and for different choices of the ratio between cosmic ray protons and electrons (k) and for different choices of the minimum energy of electrons. Bottom panel: Number of cosmic ray electrons required to explain radio halo emissions of different powers at 144 MHz, assuming $\alpha = 1.3$ and $\gamma_{\rm min} = 10$ and for $K = 1$ or $K = 100$. In both panels, we assume that the radio halo has a volume of 1^3 Mpc^3 and that the host cluster has a 10^{15} $M_\odot$ mass. The horizontal lines give the number of electrons injected by the entire population of radio galaxies in a cluster and only using a single activity burst, assuming a $\alpha = 0.8$ spectrum for all radio galaxies and either $K = 1$ or $K = 100$.

The two additional horizontal lines in each panel mark the total number of cosmic ray electrons injected by all radio galaxies present in a $10^{15} M_{\odot}$ cluster (again for the $K = 1$ or $K = 100$ extreme scenarios, and always considering $\gamma_{\rm min} = 10$). We computed this quantity based on the the same formalism outlined above, i.e., after assuming equiparition between magnetic fields and cosmic rays, but this time using the distribution of radio luminosities of cluster radio galaxies derived at 843 MHz in [120], and assuming a power-size relation from [121] to obtain the largest linear scale (LLS). From the latter, we estimate the volume occupied by radio lobes following the recent theoretical results in [122], in which the evolution of simulated FRI radio sources in idealized cluster atmospheres was studied, reporting an approximate scaling of $V_g \sim LLS^3 \cdot (10\ \mathrm{kpc/LLS})$ between the size of expanding lobes and the volume they occupy.

In essence, this simplistic model gives an idea of the number of cosmic ray electrons that can be available as a result of a single generation of radio lobes by all radio galaxies in a typical cluster. Note that since it is reasonable that the K ratio in lobes and in radio halos is the same, to a first approximation, only the lines referred to as equal K should be compared here. Using as a reference the case of a $\alpha = 1.3$ radio halo in a $10^{15}\ M_{\odot}$ cluster, the left panel shows that a single episode of activity by all radio galaxies in a cluster can easily account for all electrons required by a $\sim 5 \times 10^{30}$ –10^{31} erg/s/Hz halo at 144 MHz; while for more powerful halos, multiple burst episodes (up to $\sim$10) are required instead. The actual number of bursts from radio galaxies can be slightly lowered if the additional injection by cosmic rays by galactic winds or structure formation shocks is included, e.g., [123,124]. This simple formalism can also be extended to other kinds of diffuse sources like radio relics, yet the assumption of equipartition between cosmic rays and magnetic fields is much more questionable, owing to the much shorter acceleration timescale that is supposed to be at work in shock-accelerated cosmic rays.

Although this analysis suggests that the present and past activity by a typical population of radio galaxies in the ICM can explain the total number of electrons required to power diffuse radio sources, the actual ICM dynamics leading to the transport of cosmic rays has to be properly modeled in order to test whether the injection by radio galaxies is a viable seeding scenario to quantitatively explain observations.

Numerical Simulations

The actual transport of electrons injected by radio jets mixing with the (often turbulent) ICM can only be followed with fluid simulations, where also larger scale mixing motions induced by accretions, or by the repeated activity of AGN feedback, are included. While accounting for the full multi-scale complexity of this process is a challenge, even for modern numerical simulations, several studies have at least captured the most important pattern associated with large-scale circulation of the material ejected by jets.

Starting from the pioneering work in [125], in which the mixing of buoyant bubbles in a typical cluster environment was simulated and their radio detectability as a function of time was studied, numerical simulations have kept refining the state of the art of our understanding of how AGN feedback can affect the ICM; see, e.g., [12] for a recent review. Relatively fewer works have focused on the interplay between the remnant plasma ejected by AGN and the cluster environment, often resorting to a combination of different numerical methods in order to best capture the multi-scale nature of this process. For example, Ref. [126] used a Eulerian magneto-hydrodynamical approach to account for "cluster weather" on radio lobes expanding into the perturbed environment of a cluster of galaxies produced by a smoothed-particle hydrodynamics simulation. Likewise, the semi-analytic modeling of radio jets in [127] has been recently coupled to the Eulerian hydrodynamical re-simulation of jets crossing the ICM extracted from a large suite of SPH cosmological simulations in [128], which allowed them to probe the impressive resolution of 0.05 kpc/cell, and even to explore the potential connection with the production of "odd radio circles" in follow-up work [129].

A few studies have explored the possibility of a more direct connection between observed radio relics and the fueling by single, nearby radio galaxies, by simulating the evolution of re-accelerated fossil electrons. In a series of works, Refs. [21,130,131] modeled the formation of radio relics using 1D diffusive convection simulations with the goal of reproducing, first, the integrated radio emission spectra and the profile of radio emission across the width of real relics (e.g., the "toothbrush" in the merging cluster 1RXS J060303.3, and the "sausage" in cluster CIZA J2242.8 + 5301). In particular, they tested direct shock acceleration models, based on diffusive shock acceleration, versus models in which the radio-emitting particles were re-accelerated by weak shocks ($\mathcal{M} \leq 2$) running over a pre-existing population of fossil electrons with a low-energy cutoff ($\gamma \sim 8 \times 10^4$). The latter scenario was shown to reproduce reasonably well the observed integrated spectrum and the profile of radio surface brightness for the toothbrush, as well as the downstream curvature of the spectrum. A necessary ingredient for the model was, therefore, the presence of a wide and rather uniform distribution of "fossil" relativistic electrons, which they suggest could have been seeded by the previous activity of AGN in this sector of the cluster (e.g., Figure 3).

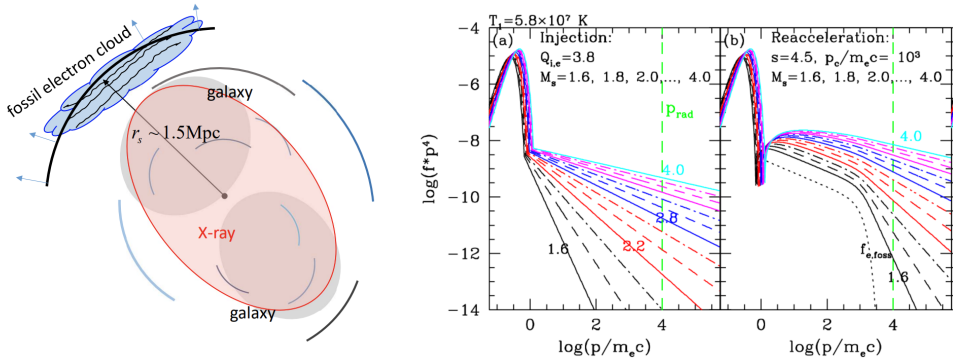

Figure 3. Left: Cartoon sketch of the bubble of fossil relativistic electrons at the location of the "sausage" radio relic in cluster CIZA J2242.8 + 5301. Centrl and right panel: electron spectra resulting from the injection of fresh electrons via diffusive shock acceleration, as a function of Mach number (central panel), and from the re-acceleration of fossil relativistic electrons by the same shocks (right panel); taken from [131].

The formation and long-term evolution of disturbed radio tails in clusters have been extensively investigated in a series of works [132–135] in which non-cosmological high-resolution MHD simulations were coupled to the simulation of the cosmic ray fluid associated with remnant plasma.

Refs. [24,136] investigated whether the morphology of some radio relics can reflect the distribution of fossil relativistic electrons previously injected by central AGN in clusters, and later dispersed into the ICM by sloshing gas motions generated by a previous merger event. They found that the transport of electrons along a spiral path, and its stretching tangentially to the spiral pattern, could produce a filamentary emission pattern compatible with real radio relics (see, e.g., Figure 4). Following this approach, Ref. [89] proposed a similar scenario to model the filamentary diffuse radio emission in Abel 2657 out of a shredded AGN bubble.

Recently, Ref. [79] produced high-resolution MHD simulations to model the complex radio structure in A3376, in which they accounted for the interaction between an AGN jet and a curved ICM magnetic field. They showed that the simulated jet propagation is quenched by the magnetic tension, which induces a later escape of the flow and of the relativistic particles carried with it, which can reasonably mimic the sharp "double-scythe" shape of the real observation. The magnetic field which best reproduces the synchrotron morphology is of order ∼10 μG, and the modeling suggests that magnetic reconnection might additionally be at work to produce an efficient injection of cosmic rays in the region.

However, whether a single burst from AGN combined with turbulence and mixing motions in clusters can provide a sufficient seeding of relativistic electrons to cover the entire extent of observed radio relics is not a fully settled issue.

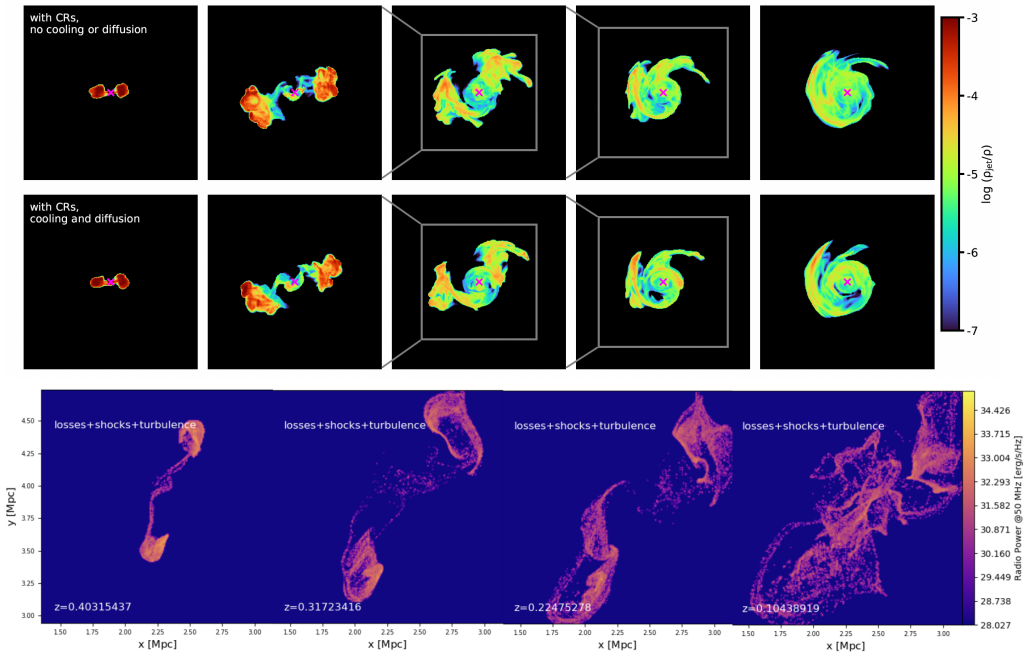

Figure 4. Top panels: Evolution of the projected density of fluid tracers ejected by AGN-inflated bubbles in simulations in [136]. The top row shows the evolution in the case in which cosmic rays are passively advected with the fluid, while in the lower row the effects of cosmic ray diffusion and Alfvén losses are included. Last row: Projected synchrotron radio emission at 150 MHz and for four different evolutionary steps, for a simulated pair of bubbles inflated by an AGN in the cosmological simulation in [137], in which electrons could age by radiative processes, as well as be re-energized by shocks and turbulent re-acceleration.

To explore this question, Refs. [137,138] modeled the dynamics of radio jets mixing with the turbulent ICM in cosmological simulations, while also following the spatial and spectral energy evolution of fossil electrons injected by AGN sources (see bottom panels of Figure 4). Their simulations showed that right after the active stage of radio jets, the buoyant stage of mixing of relativistic electrons is soon followed by a longer stage of large-scale mixing driven by turbulent motions in the ICM. During that phase, the remnant radio plasma can remain detectable at low frequencies out to $\leq$0.5 Mpc distance from sources, and even up to $\sim$0.5–1 Gyr since its first injection, provided that re-acceleration from weak shocks or turbulence is triggered by the cluster accretion dynamics. The emission from re-accelerated fossil electrons can produce detectable emission at any time, but it can typically produce only small ($\leq$100 kpc) and often filamentary radio features with steep radio spectra ($\alpha \geq$ 1.5–2). With the same approach, Ref. [139] studied the mixing of electrons injected by eight realistic radio sources all activated at once in the same cluster, and compared their efficiency in seeding the ICM with cosmic rays to shocks driven by mergers in the same cluster, finding that the latter more naturally generate a volume-filling distribution of fossil electrons on the scales typically covered by radio relics, as also reported by other complementary analyses [140,141].

A common prediction from all of the aforementioned numerical approaches is that the detectable structures associated with plasma tails or remnant plasma from radio galaxies can only probe "the tip of the iceberg" of a broader and more volume-filling distribution of fossil electrons. To visualize this, we show in Figure 5 the measured evolution of the area-filling factor, $\Psi(2D)$, of the radio emission from the same simulation by [139], where eight radio galaxies release magnetic jets in a $\sim 10^{14}$ $M_{\odot}$ galaxy cluster, all at $z = 0.5$ and

with a range of realistic jet powers. In the figure, we show the fraction of area of radial shells from the cluster center which is visible at different radio frequencies (50, 140, 610, and 1400 MHz), assuming for simplicity a detection threshold which scales with frequency as $\sigma(\nu) = \sigma_{LBA}[\nu/(50\ \mathrm{MHz})]^{-1}$, where $\sigma_{LBA} = \sigma = 5.7 \cdot 10^{-4}$ Jy/beam, as in, e.g., [32], assuming a beam of $\theta = 12.5''$ and a (non-evolving) luminosity distance of the cluster of $d_L = 132$ Mpc. The additional gray dotted lines in each panel show instead the area-covering factor of the entire distribution of cosmic ray electrons injected by simulated radio galaxies, projected along the same line of sight. Of course, while the area-filling factor of electrons mixing in the ICM can be large, the filling factor of the detectable radio emission can be much smaller, because it depends on the fraction of relativistic electrons in the high-energy tail of the distribution, as well as on the observing frequency, and it varies with the available sensitivity of each radio observation. In particular, given the same volume-filling distribution of relativistic electrons released by radio galaxies (or other mechanisms), different scenarios for the energy evolution of such electrons can vary their observable area-filling factor at different radio wavelengths. As can be seen, the area-filling factor of the observable emission rapidly drops with time, at an increased rate for higher frequencies. At a time of $\sim$1.2 Gyr after their injection in the cluster, the electrons from all galaxies have spread to large radii, due to the combined effect of the initial jet velocity of the large-scale turbulent motions in the cluster, which can reach $\sigma_v \sim 300$ km/s in this simulated cluster [138]. However, cosmic rays dilute as they expand into the cluster volume, and $\sim$0.25 Gyr after the injection less than $\sim$30% of the projected area at $\sim 0.5\ R_{200}$ is covered by cosmic rays, which further declines to $\sim$20% 1 Gyr later. At this epoch, less than $\sim$5% of the projected area at $\sim R_{200}$ is covered by cosmic rays along the line of sight. The area-covering factor of the observable emission drops sharply with frequency and time: already $\sim$0.25 Gyr since the jets' injection, $\sim$30% of the surface at $\sim 0.5\ R_{200}$ is detectable at 50 MHz, but less than $\sim$5% at 1400 MHz. One Gyr later, there is virtually no detectable emission from the remnant plasma from jets beyond $\sim 0.4\ R_{200}$, and the very steep spectral energy distribution makes a detection only possible for low-frequency ($\leq$140 MHz) radio observations within that radius. It should be noted that this modeling cannot capture the additional effect of cosmic ray diffusion in the tangled ICM magnetic field, which can surely increase the volume-filling factor of cosmic rays. However, the timescales of the spatial diffusion of cosmic ray electrons are much longer than the evolutionary range considered here. In the range of energy of interest here, the diffusion coefficient should be in the $D \leq 10^{30} \sim 10^{31}$ cm^2/s ballpark, e.g., [25] and discussion therein, which means that the diffusion timescale over a $L \approx 1$ Mpc scale is $\tau_{\mathrm{diff}} \sim L^2/(4D) \geq 7.5$–$75$ Gyr, and hence, is a a very slow and sub-dominant mechanism.

In summary, in line with the simplistic theoretical derivation of the previous section, the repeated activity of a few radio galaxies in clusters ($\leq$10), together with the typical turbulent gas motions expected from numerical simulations, appears sufficient to fill most of the area covered by observed radio halos ($\leq 0.1\ R_{200}$) with relativistic electrons.

On the other hand, the external regions where radio relics typically form ($\geq 0.5\ R_{200}$, e.g., [142,143]) are hardly replenished by a significant amount of fossil cosmic ray electrons, even by multiple radio galaxies, and probably additional cluster wide motions (e.g., sloshing) are required to conveniently distribute the remnant plasma in a more uniform way, before shocks revive it, as already suggested, e.g., [24]. How common the appearance of such configurations is in the lifetime of clusters of galaxies remains to be assessed. Complementary to this, the injection of cosmic rays by merger shocks can naturally lead to large and correlated populations of fossil electrons that subsequent re-acceleration events can illuminate on $\sim$Mpc scales [22,139–141], and moreover, the ubiquitous presence of turbulent motions, even in the outskirts of the cluster, can maintain electrons at a higher energy than expected only considering the effect of radiative losses, i.e., up to $\gamma \sim 10^3$ [35]. This would imply the existence of a second and rather uniform population of fossil electrons on larger cluster scales, in addition to the outcome of evolving radio cluster galaxies.

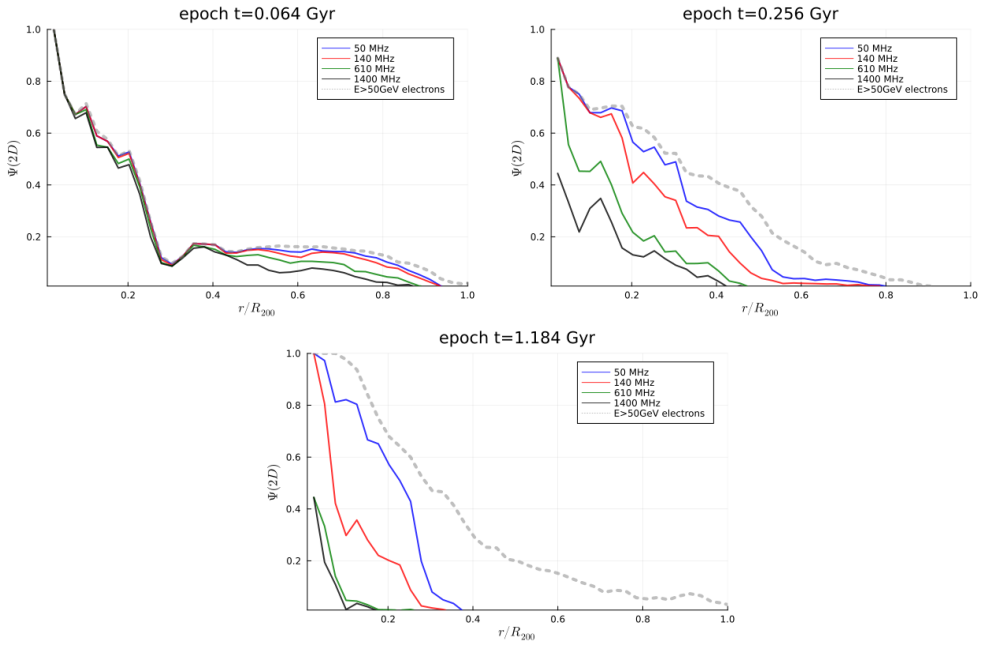

Figure 5. Area-filling factors of detectable radio emission as a function of frequency (different colors) and of relativistic electrons (dotted gray lines) for three different epochs since the injection of radio jets in the cosmological simulation by [139].

4. Conclusions and Future Perspectives

In summary, both the direct observations of remnant radio plasma and of disturbed radio tails, and the more indirect indications of a connection between the activity of radio galaxies and large diffuse radio emissions in clusters of galaxies (i.e., radio halos and radio relics) support the idea that the fueling of relativistic electrons from cluster radio galaxies is a key process to regulate the non-thermal energy budget of the ICM.

From the theoretical viewpoint, the time-integrated activity of the population of radio galaxies in clusters appear sufficient to fuel the entire extent of diffuse radio emissions with the necessary amount of fossil electrons, while the exact timescales and efficiency with which relativistic electrons spread across the ICM depend on the multi-scale gas dynamics, and its investigation with modern numerical methods has just begun. Observations at very low frequencies (<100 MHz) performed with LOFAR2.0 and SKA-LOW will soon make it possible to recover the emission from older populations of cosmic ray electrons in the ICM. In parallel, with the excellent polarization capabilities of the new generation of radio telescopes (e.g., MeerKAT+, SKA-MID), these instruments will allow the investigation of highly inefficient re-energization processes sustaining particle lifetimes in the ICM.

Among the main processes to re-accelerate fossil electrons in the ICM, shocks and turbulence are the dominant mechanisms. While the detection of shock fronts has been already enabled by instruments such as *Chandra*, *XMM-Newton*, and *Suzaku*, the direct observation of turbulent motions is limited to the case of Perseus by Hitomi [144]. The deployment of new X-ray facilities capable of measuring the gas turbulent motions, either with a large integration area (e.g., *XRISM*) or in a more spatially resolved manner (e.g., *Athena*), promises to enable better constraints to be provided on the multi-scale dynamical interactions between the relativistic plasma dispersed by radio galaxies, and the evolving ICM.

Author Contributions: F.V. and A.B. curated the manuscript, the figures and the interpretation of results in equal parts. All authors have read and agreed to the published version of the manuscript.

Funding: F.V. acknowledges partial financial support from the Cariplo "BREAKTHRU" funds Rif: 2022-2088 CUP J33C22004310003. A.B. acknowledges financial support from the European Union-Next Generation EU.

Acknowledgments: The authors thank Annalisa Bonafede, Marisa Brienza, Hyesung Kang, Wonki Lee, Ramij Raja, Kamlesh Rajpurohit and John ZuHone for the kind permission to reuse the figures of their papers for this work. We thank Lawrence Rudnick for his constructive feedback on the manuscript, as well as our anonymous reviewers.

Conflicts of Interest: The authors declare no conflicts of interest.

Abbreviations

The following abbreviations are used in this manuscript:

AGN	Active galactic nucleus
AMR	Adaptive mesh refinement
ASKAP	Australian Square Kilometre Array Pathfinder
BCG	Brightest central galaxy
DSA	Diffusive shock acceleration
GReET	Gently re-energized tail
HBA	High-band antenna
HT	Head–tail
ICM	Intracluster medium
LBA	Low-band antenna
LLS	Largest linear scale
LOFAR	Low Frequency Array
MHD	Magnetohydro dynamics
MWA	Murchison Widefield Array
NAT	Narrow-angle tail
SMBH	Super massive black hole
SPH	Smoothed-particle Hydrodynamics
WAT	Wide-angle tail
ΛCDM	Lambda cold dark matter

References

1. Croston, J.H.; Hardcastle, M.J.; Birkinshaw, M.; Worrall, D.M.; Laing, R.A. An XMM-Newton study of the environments, particle content and impact of low-power radio galaxies. *Mon. Not. R. Astron. Soc.* **2008**, *386*, 1709–1728. [CrossRef]
2. Croston, J.H.; Ineson, J.; Hardcastle, M.J. Particle content, radio-galaxy morphology, and jet power: All radio-loud AGN are not equal. *Mon. Not. R. Astron. Soc.* **2018**, *476*, 1614–1623. [CrossRef]
3. Norman, M.L.; Bryan, G.L. Cluster Turbulence. In Proceedings of the Radio Galaxy Messier 87,Tegernsee, Germany, 15–19 September 1997; Röser, H.-J., Meisenheimer, K., Eds.; Springer: Berlin/Heidelberg, Germany, 1999; Volume 530, pp. 106–115. [CrossRef]
4. Dolag, K.; Vazza, F.; Brunetti, G.; Tormen, G. Turbulent gas motions in galaxy cluster simulations: The role of smoothed particle hydrodynamics viscosity. *Mon. Not. R. Astron. Soc.* **2005**, *364*, 753–772. [CrossRef]
5. Vazza, F.; Brunetti, G.; Gheller, C.; Brunino, R.; Brüggen, M. Massive and refined. II. The statistical properties of turbulent motions in massive galaxy clusters with high spatial resolution. *Astron. Astrophys.* **2011**, *529*, A17. [CrossRef]
6. Schmidt, W.; Byrohl, C.; Engels, J.F.; Behrens, C.; Niemeyer, J.C. Viscosity, pressure and support of the gas in simulations of merging cool-core clusters. *Mon. Not. R. Astron. Soc.* **2017**, *470*, 142–156. [CrossRef]
7. Ayromlou, M.; Nelson, D.; Pillepich, A.; Rohr, E.; Truong, N.; Li, Y.; Simionescu, A.; Lehle, K.; Lee, W. An Atlas of Gas Motions in the TNG-Cluster Simulation: From Cluster Cores to the Outskirts. *arXiv* **2023**, arXiv:2311.06339.
8. Churazov, E.; Forman, W.; Jones, C.; Sunyaev, R.; Böhringer, H. XMM-Newton observations of the Perseus cluster-II. Evidence for gas motions in the core. *Mon. Not. R. Astron. Soc.* **2004**, *347*, 29–35. [CrossRef]
9. Heinz, S.; Brüggen, M.; Young, A.; Levesque, E. The answer is blowing in the wind: Simulating the interaction of jets with dynamic cluster atmospheres. *Mon. Not. R. Astron. Soc.* **2006**, *373*, L65–L69. [CrossRef]
10. Gaspari, M.; Ruszkowski, M.; Sharma, P. Cause and Effect of Feedback: Multiphase Gas in Cluster Cores Heated by AGN Jets. *Astrophys. J.* **2012**, *746*, 94. [CrossRef]
11. Li, Y.; Bryan, G.L. Modeling Active Galactic Nucleus Feedback in Cool-core Clusters: The Balance between Heating and Cooling. *Astrophys. J.* **2014**, *789*, 54. [CrossRef]
12. Bourne, M.A.; Yang, H.Y.K. Recent Progress in Modeling the Macro- and Micro-Physics of Radio Jet Feedback in Galaxy Clusters. *Galaxies* **2023**, *11*, 73. [CrossRef]
13. Völk, H.J.; Atoyan, A.M. Early Starbursts and Magnetic Field Generation in Galaxy Clusters. *Astrophys. J.* **2000**, *541*, 88–94. [CrossRef]
14. Hardcastle, M.J.; Croston, J.H. Radio galaxies and feedback from AGN jets. *New Astron. Rev.* **2020**, *88*, 101539. [CrossRef]

15. de Gasperin, F.; Intema, H.T.; Shimwell, T.W.; Brunetti, G.; Brüggen, M.; Enßlin, T.A.; van Weeren, R.J.; Bonafede, A.; Röttgering, H.J.A. Gentle reenergization of electrons in merging galaxy clusters . *Sci. Adv.* **2017**, *3*, e1701634. [CrossRef]
16. Wilber, A.; Brüggen, M.; Bonafede, A.; Savini, F.; Shimwell, T.; van Weeren, R.J.; Rafferty, D.; Mechev, A.P.; Intema, H.; Andrade-Santos, F.; et al. LOFAR discovery of an ultra-steep radio halo and giant head-tail radio galaxy in Abell 1132 . *Mon. Not. R. Astron. Soc.* **2018**, *473*, 3536–3546. [CrossRef]
17. Mandal, S.; Intema, H.T.; van Weeren, R.J.; Shimwell, T.W.; Botteon, A.; Brunetti, G.; de Gasperin, F.; Brüggen, M.; Di Gennaro, G.; Kraft, R.; et al. Revived fossil plasma sources in galaxy clusters . *Astron. Astrophys.* **2020**, *634*, A4. [CrossRef]
18. Quici, B.; Turner, R.J.; Seymour, N.; Hurley-Walker, N.; Shabala, S.S.; Ishwara-Chandra, C.H. Selecting and modelling remnant AGNs with limited spectral coverage. *Mon. Not. R. Astron. Soc.* **2022**, *514*, 3466–3484. [CrossRef]
19. Brienza, M.; Lovisari, L.; Rajpurohit, K.; Bonafede, A.; Gastaldello, F.; Murgia, M.; Vazza, F.; Bonnassieux, E.; Botteon, A.; Brunetti, G.; et al. The galaxy group NGC 507: Newly detected AGN remnant plasma transported by sloshing. *Astron. Astrophys.* **2022**, *661*, A92. [CrossRef]
20. van Weeren, R.J.; de Gasperin, F.; Akamatsu, H.; Brüggen, M.; Feretti, L.; Kang, H.; Stroe, A.; Zandanel, F. Diffuse Radio Emission from Galaxy Clusters. *Sci. Space Rev.* **2019**, *215*, 16. [CrossRef]
21. Kang, H.; Ryu, D.; Jones, T.W. Diffusive Shock Acceleration Simulations of Radio Relics. *Astrophys. J.* **2012**, *756*, 97. [CrossRef]
22. Pinzke, A.; Oh, S.P.; Pfrommer, C. Giant radio relics in galaxy clusters: Reacceleration of fossil relativistic electrons? *Mon. Not. R. Astron. Soc.* **2013**, *435*, 1061–1082. [CrossRef]
23. Botteon, A.; Brunetti, G.; Ryu, D.; Roh, S. Shock acceleration efficiency in radio relics. *Astron. Astrophys.* **2020**, *634*, A64. [CrossRef]
24. ZuHone, J.A.; Markevitch, M.; Weinberger, R.; Nulsen, P.; Ehlert, K. How Merger-driven Gas Motions in Galaxy Clusters Can Turn AGN Bubbles into Radio Relics. *Astrophys. J.* **2021**, *914*, 73. [CrossRef]
25. Brunetti, G.; Jones, T.W. Cosmic Rays in Galaxy Clusters and Their Nonthermal Emission. *Int. J. Mod. Phys. D* **2014**, *23*, 1430007. [CrossRef]
26. Cassano, R.; Gitti, M.; Brunetti, G. A morphological comparison between giant radio halos and radio mini-halos in galaxy clusters. *Astron. Astrophys.* **2008**, *486*, L31–L34. [CrossRef]
27. Richard-Laferrière, A.; Hlavacek-Larrondo, J.; Nemmen, R.S.; Rhea, C.L.; Taylor, G.B.; Prasow-Émond, M.; Gendron-Marsolais, M.; Latulippe, M.; Edge, A.C.; Fabian, A.C.; et al. On the relation between mini-halos and AGN feedback in clusters of galaxies. *Mon. Not. R. Astron. Soc.* **2020**, *499*, 2934–2958. [CrossRef]
28. Govoni, F.; Orrù, E.; Bonafede, A.; Iacobelli, M.; Paladino, R.; Vazza, F.; Murgia, M.; Vacca, V.; Giovannini, G.; Feretti, L.; et al. A radio ridge connecting two galaxy clusters in a filament of the cosmic web. *Science* **2019**, *364*, 981–984. [CrossRef]
29. Brunetti, G.; Vazza, F. Second-order Fermi Reacceleration Mechanisms and Large-Scale Synchrotron Radio Emission in Intracluster Bridges. *Phys. Rev. Lett.* **2020**, *124*, 051101. [CrossRef]
30. de Jong, J.; van Weeren, R.J.; Botteon, A.; Oonk, J.; Brunetti, G.; Shimwell, T.W.; Cassano, R.; Röttgering, H.J.; Tasse, C. Deep study of A399-401: Application of a wide-field facet calibration. *Astron. Astrophys.* **2022**, *668*, A107. [CrossRef]
31. Shweta, A.; Athreya, R.M.; Sekhar, S. Reenergization of Radio Halo Electrons in the Merging Galaxy Cluster A2163 . *Astrophys. J.* **2020**, *897*, 115. [CrossRef]
32. Botteon, A.; van Weeren, R.J.; Brunetti, G.; Vazza, F.; Shimwell, T.W.; Brüggen, M.; Röttgering, H.J.; de Gasperin, F.; Akamatsu, H.; Bonafede, A.; et al. Magnetic fields and relativistic electrons fill entire galaxy cluster. *Sci. Adv.* **2022**, *8*, eabq7623. [CrossRef] [PubMed]
33. Cuciti, V.; de Gasperin, F.; Brüggen, M.; Vazza, F.; Brunetti, G.; Shimwell, T.W.; Edler, H.W.; van Weeren, R.J.; Botteon, A.; Cassano, R.; et al. Galaxy clusters enveloped by vast volumes of relativistic electrons. *Nature* **2022**, *609*, 911–914. [CrossRef] [PubMed]
34. Bruno, L.; Botteon, A.; Shimwell, T.W.; Cuciti, V.; de Gasperin, F.; Brunetti, G.; Dallacasa, D.; Gastaldello, F.; Rossetti, M.; van Weeren, R.J.; et al. A three-component giant radio halo: The puzzling case of the galaxy cluster Abell 2142. *Astron. Astrophys.* **2023**, *678*, A133. [CrossRef]
35. Beduzzi, L.; Vazza, F.; Brunetti, G.; Cuciti, V.; Wittor, D.; Corsini, E. Exploring the origins of mega radio halos. *Astron. Astrophys.* **2023**, *678*, L8. [CrossRef]
36. Nishiwaki, K.; Asano, K.; Murase, K. High-energy Neutrino Constraints on Cosmic-Ray Reacceleration in Radio Halos of Massive Galaxy Clusters. *Astrophys. J.* **2023**, *954*, 188. [CrossRef]
37. Lee, W.; ZuHone, J.A.; James Jee, M.; HyeongHan, K.; Kale, R.; Ahn, E. Discovery of A Large-scale Bent Radio Jet in the Merging Cluster A514. *Astrophys. J.* **2023**, *957*, L4. [CrossRef]
38. Raja, R.; Rahaman, M.; Datta, A.; Smirnov, O.M. A Multi-Frequency View of the Radio Phoenix in the Abell 85 Cluster. *arXiv* **2023**, arXiv:2309.14244.
39. Botteon, A.; Brunetti, G.; van Weeren, R.J.; Shimwell, T.W.; Pizzo, R.F.; Cassano, R.; Iacobelli, M.; Gastaldello, F.; Bîrzan, L.; Bonafede, A.; et al. The Beautiful Mess in Abell 2255. *Astrophys. J.* **2020**, *897*, 93. [CrossRef]
40. Rajpurohit, K.; Osinga, E.; Brienza, M.; Botteon, A.; Brunetti, G.; Forman, W.R.; Riseley, C.J.; Vazza, F.; Bonafede, A.; van Weeren, R.J.; et al. Deep low-frequency radio observations of Abell 2256. II. The ultra-steep spectrum radio halo. *Astron. Astrophys.* **2023**, *669*, A1. [CrossRef]
41. Bonafede, A.; Brunetti, G.; Rudnick, L.; Vazza, F.; Bourdin, H.; Giovannini, G.; Shimwell, T.W.; Zhang, X.; Mazzotta, P.; Simionescu, A.; et al. The Coma Cluster at LOFAR Frequencies. II. The Halo, Relic, and a New Accretion Relic. *Astrophys. J.* **2022**, *933*, 218. [CrossRef]

42. Kempner, J.C.; Blanton, E.L.; Clarke, T.E.; Enßlin, T.A.; Johnston-Hollitt, M.; Rudnick, L. Conference Note: A Taxonomy of Extended Radio Sources in Clusters of Galaxies. In Proceedings of the Riddle of Cooling Flows in Galaxies and Clusters of Galaxies, Charlottesville, VA, USA, 31 May–4 June 2003; Reiprich, T., Kempner, J., Soker, N., Eds.; p. 335.
43. Slee, O.; Reynolds, J. Steep-spectrum radio sources in clusters of galaxies - the southern sample. *Publ. Astron. Soc. Aust.* **1984**, *5*, 516–529. [CrossRef]
44. Slee, O.; Roy, A. An extreme example of a radio relic in Abell 4038. *Mon. Not. R. Astron. Soc.* **1998**, *297*, L86–L92. [CrossRef]
45. Slee, O.; Roy, A.; Murgia, M.; Andernach, H.; Ehle, M. Four Extreme Relic Radio Sources in Clusters of Galaxies. *Astron. J.* **2001**, *122*, 1172–1193. [CrossRef]
46. Subrahmanyan, R.; Beasley, A.; Goss, W.; Golap, K.; Hunstead, R.W. PKS B1400-33: An Unusual Radio Relic in a Poor Cluster. *Astron. J.* **2003**, *125*, 1095–1106. [CrossRef]
47. Green, D.A.; Lacy, M.; Bhatnagar, S.; Gates, E.; Warner, P. Radio and near-infrared observations of the steep-spectrum Galactic plane radio source WKB 0314+57.8. *Mon. Not. R. Astron. Soc.* **2004**, *354*, 1159–1164. [CrossRef]
48. Duchesne, S.W.; Johnston-Hollitt, M.; Zhu, Z.H.; Wayth, R.; Line, J. Murchison Widefield Array detection of steep-spectrum, diffuse, non-thermal radio emission within Abell 1127. *Publ. Astron. Soc. Aust.* **2020**, *37*, e037. [CrossRef]
49. Botteon, A.; Giacintucci, S.; Gastaldello, F.; Venturi, T.; Brunetti, G.; van Weeren, R.J.; Shimwell, T.W.; Rossetti, M.; Akamatsu, H.; Brüggen, M.; et al. Nonthermal phenomena in the center of Abell 1775. An 800 kpc head-tail, revived fossil plasma and slingshot radio halo. *Astron. Astrophys.* **2021**, *649*, A37. [CrossRef]
50. Hodgson, T.; Bartalucci, I.; Johnston-Hollitt, M.; McKinley, B.; Vazza, F.; Wittor, D. Ultra-steep-spectrum Radio "Jellyfish" Uncovered in A2877. *Astrophys. J.* **2021**, *909*, 198. [CrossRef]
51. Pandge, M.; Sebastian, B.; Seth, R.; Raychaudhury, S. A detailed study of X-ray cavities in the intracluster environment of the cool core cluster Abell 3017. *Mon. Not. R. Astron. Soc.* **2021**, *504*, 1644–1656. [CrossRef]
52. Pandge, M.; Kale, R.; Dabhade, P.; Mahato, M.; Raychaudhury, S. Giant Metrewave Radio Telescope unveils steep-spectrum antique filaments in the galaxy cluster Abell 725. *Mon. Not. R. Astron. Soc.* **2022**, *509*, 1837–1847. [CrossRef]
53. Pasini, T.; Edler, H.; Brüggen, M.; de Gasperin, F.; Botteon, A.; Rajpurohit, K.; van Weeren, R.J.; Gastaldello, F.; Gaspari, M.; Brunetti, G.; et al. Particle re-acceleration and diffuse radio sources in the galaxy cluster Abell 1550. *Astron. Astrophys.* **2022**, *663*, A105. [CrossRef]
54. Riseley, C.J.; Bonnassieux, E.; Vernstrom, T.; Galvin, T.; Chokshi, A.; Botteon, A.; Rajpurohit, K.; Duchesne, S.W.; Bonafede, A.; Rudnick, L.; et al. Radio fossils, relics, and haloes in Abell 3266: Cluster archaeology with ASKAP-EMU and the ATCA. *Mon. Not. R. Astron. Soc.* **2022**, *515*, 1871–1896. [CrossRef]
55. Groenveld, C.; van Weeren, R.J.; Osinga, E.; Williams, W.L.; Callingham, J.R.; de Gasperin, F.; Botteon, A.; Shimwell, T.; Swejen, F.; de Jong, J.M.G.H.J.; et al. Characterisation of the decameter sky at sub-arcminute resolution. *Nat. Astron.* **2024** , *accepted*.
56. Mandal, S.; Intema, H.T.; Shimwell, T.W.; van Weeren, R.J.; Botteon, A.; Röttgering, H.J.; Hoang, D.N.; Brunetti, G.; de Gasperin, F.; Giacintucci, S.; et al. Ultra-steep spectrum emission in the merging galaxy cluster Abell 1914. *Astron. Astrophys.* **2019**, *622*, A22. [CrossRef]
57. Juett, A.; Sarazin, C.L.; Clarke, T.E.; Andernach, H.; Ehle, M.; Fujita, Y.; Kempner, J.C.; Roy, A.; Rudnick, L.; Slee, O. A Chandra Observation of Abell 13: Investigating the Origin of the Radio Relic. *Astrophys. J.* **2008**, *672*, 138–145. [CrossRef]
58. Owen, F.N.; Rudnick, L.; Eilek, J.A.; Rau, U.; Bhatnagar, S.; Kogan, L. Wideband Very Large Array Observations of A2256. I. Continuum, Rotation Measure, and Spectral Imaging. *Astrophys. J.* **2014**, *794*, 24. [CrossRef]
59. Werner, N.; Zhuravleva, I.; Canning, R.E.; Allen, S.W.; King, A.; Sanders, J.S.; Simionescu, A.; Taylor, G.B.; Morris, R.G.; Fabian, A.C. Deep Chandra study of the truncated cool core of the Ophiuchus cluster. *Mon. Not. R. Astron. Soc.* **2016**, *460*, 2752–2764. [CrossRef]
60. van Weeren, R.J.; Shimwell, T.W.; Botteon, A.; Brunetti, G.; Brüggen, M.; Boxelaar, J.M.; Cassano, R.; Di Gennaro, G.; Andrade-Santos, F.; Bonnassieux, E.; et al. LOFAR observations of galaxy clusters in HETDEX. Extraction and self-calibration of individual LOFAR targets. *Astron. Astrophys.* **2021**, *651*, A115. [CrossRef]
61. Duchesne, S.W.; Johnston-Hollitt, M.; Offringa, A.R.; Pratt, G.W.; Zheng, Q.; Dehghan, S. Diffuse galaxy cluster emission at 168 MHz within the Murchison Widefield Array Epoch of Reionization 0-h field. *Publ. Astron. Soc. Aust.* **2021**, *38*, e010. [CrossRef]
62. Duchesne, S.W.; Johnston-Hollitt, M.; Bartalucci, I. Low-frequency integrated radio spectra of diffuse, steep-spectrum sources in galaxy clusters: Palaeontology with the MWA and ASKAP. *Publ. Astron. Soc. Aust.* **2021**, *38*, e053. [CrossRef]
63. Botteon, A.; Shimwell, T.W.; Cassano, R.; Cuciti, V.; Zhang, X.; Bruno, L.; Camillini, L.; Natale, R.; Jones, A.; Gastaldello, F.; et al. The Planck clusters in the LOFAR sky. I. LoTSS-DR2: New detections and sample overview. *Astron. Astrophys.* **2022**, *660*, A78. [CrossRef]
64. Hoang, D.N.; Brüggen, M.; Botteon, A.; Shimwell, T.W.; Zhang, X.; Bonafede, A.; Bruno, L.; Bonnassieux, E.; Cassano, R.; Cuciti, V.; et al. Diffuse radio emission from non-Planck galaxy clusters in the LoTSS-DR2 fields. *Astron. Astrophys.* **2022**, *665*, A60. [CrossRef]
65. Knowles, K.; Cotton, W.; Rudnick, L.; Camilo, F.; Goedhart, S.; Deane, R.; Ramatsoku, M.; Bietenholz, M.; Brüggen, M.; Button, C.; et al. The MeerKAT Galaxy Cluster Legacy Survey. I. Survey Overview and Highlights. *Astron. Astrophys.* **2022**, *657*, A56. [CrossRef]

66. Duchesne, S.W.; Botteon, A.; Koribalski, B.S.; Loi, F.; Rajpurohit, K.; Riseley, C.J.; Rudnick, L.; Vernstrom, T.; Andernach, H.; Hopkins, A.M.; et al. Evolutionary Map of the Universe (EMU): A pilot search for diffuse, non-thermal radio emission in galaxy clusters with the Australian SKA Pathfinder. *arXiv* **2024**, arXiv:2402.06192.
67. Miley, G.K. The structure of extended extragalactic radio sources. *Annu. Rev. Astron. Astrophys.* **1980**, *18*, 165–218. [CrossRef]
68. Sarazin, C.L. The energy spectrum of primary cosmic-ray electrons in clusters of galaxies and inverse compton emission. *Astrophys. J.* **1999**, *520*, 529–547. [CrossRef]
69. Sebastian, B.; Lal, D.V.; Pramesh Rao, A. Giant Metrewave Radio Telescope Observations of Head-Tail Radio Galaxies. *Astron. J.* **2017**, *154*, 169. [CrossRef]
70. Cuciti, V.; Brunetti, G.; van Weeren, R.J.; Bonafede, A.; Dallacasa, D.; Cassano, R.; Venturi, T.; Kale, R. New giant radio sources and underluminous radio halos in two galaxy clusters. *Astron. Astrophys.* **2018**, *609*, A61. [CrossRef]
71. Edler, H.; de Gasperin, F.; Brunetti, G.; Botteon, A.; Cuciti, V.; van Weeren, R.J.; Cassano, R.; Shimwell, T.W.; Brüggen, M.; Drabent, A. Abell 1033: Radio halo and gently reenergized tail at 54 MHz. *Astron. Astrophys.* **2022**, *666*, A3. [CrossRef]
72. van Weeren, R.J.; Röttgering, H.J.; Rafferty, D.; Pizzo, R.F.; Bonafede, A.; Brüggen, M.; Brunetti, G.; Ferrari, C.; Orrù, E.; Heald, G.; et al. First LOFAR observations at very low frequencies of cluster-scale non-thermal emission: The case of Abell 2256. *Astron. Astrophys.* **2012**, *543*, A43. [CrossRef]
73. Srivastava, S.; Singal, A.K. GMRT observations of IC 711-the longest head-tail radio galaxy known. *Mon. Not. R. Astron. Soc.* **2020**, *493*, 3811–3824. [CrossRef]
74. Venturi, T.; Giacintucci, S.; Merluzzi, P.; Bardelli, S.; Busarello, G.; Dallacasa, D.; Sikhosana, S.P.; Marvil, J.; Smirnov, O.M.; Bourdin, H.; et al. Radio footprints of a minor merger in the Shapley Supercluster: From supercluster down to galactic scales. *Astron. Astrophys.* **2022**, *660*, A81. [CrossRef]
75. Ignesti, A.; Brunetti, G.; Shimwell, T.W.; Gitti, M.; Bîrzan, L.; Botteon, A.; Brüggen, M.; de Gasperin, F.; Di Gennaro, G.; Edge, A.C.; et al. A LOFAR view into the stormy environment of the galaxy cluster 2A0335+096. *Astron. Astrophys.* **2022**, *659*, A20. [CrossRef]
76. Lusetti, G.; de Gasperin, F.; Cuciti, V.; Brüggen, M.; Spinelli, C.; Edler, H.; Brunetti, G.; van Weeren, R.J.; Botteon, A.; Di Gennaro, G.; et al. Re-energization of AGN head-tail radio galaxies in the galaxy cluster ZwCl 0634.1+47474. *Mon. Not. R. Astron. Soc.* **2024**, *528*, 141–159. [CrossRef]
77. van Weeren, R.J.; Andrade-Santos, F.; Dawson, W.A.; Golovich, N.R.; Lal, D.V.; Kang, H.; Ryu, D.; Brüggen, M.; Ogrean, G.; Forman, W.R.; et al. The case for electron re-acceleration at galaxy cluster shocks. *Nat. Astron.* **2017**, *1*, 5. [CrossRef]
78. Lal, D.V. NGC 4869 in the Coma Cluster: Twist, Wrap, Overlap, and Bend. *Astron. J.* **2020**, *160*, 161. [CrossRef]
79. Chibueze, J.O.; Sakemi, H.; Ohmura, T.; Machida, M.; Akamatsu, H.; Akahori, T.; Nakanishi, H.; Parekh, V.; van Rooyen, R.; Takeuchi, T.T. Jets from MRC 0600-399 bent by magnetic fields in the cluster Abell 3376. *Nature* **2021**, *593*, 47–50. [CrossRef] [PubMed]
80. Giacintucci, S.; Venturi, T.; Markevitch, M.; Bourdin, H.; Mazzotta, P.; Merluzzi, P.; Dallacasa, D.; Bardelli, S.; Sikhosana, S.P.; Smirnov, O.M.; et al. A Candle in the Wind: A Radio Filament in the Core of the A3562 Galaxy Cluster. *Astrophys. J.* **2022**, *934*, 49. [CrossRef]
81. Pfrommer, C.; Jones, T.W. Radio Galaxy NGC 1265 Unveils the Accretion Shock Onto the Perseus Galaxy Cluster. *Astrophys. J.* **2011**, *730*, 22. [CrossRef]
82. Botteon, A.; Shimwell, T.W.; Bonafede, A.; Dallacasa, D.; Gastaldello, F.; Eckert, D.; Brunetti, G.; Venturi, T.; van Weeren, R.J.; Mandal, S.; et al. The spectacular cluster chain Abell 781 as observed with LOFAR, GMRT, and XMM-Newton. *Astron. Astrophys.* **2019**, *622*, A19. [CrossRef]
83. Wilber, A.G.; Brüggen, M.; Bonafede, A.; Rafferty, D.; Shimwell, T.W.; van Weeren, R.J.; Akamatsu, H.; Botteon, A.; Savini, F.; Intema, H.T.; et al. Evolutionary phases of merging clusters as seen by LOFAR. *Astron. Astrophys.* **2019**, *622*, A25. [CrossRef]
84. Gendron-Marsolais, M.L.; Hull, C.; Perley, R.A.; Rudnick, L.; Kraft, R.P.; Hlavacek-Larrondo, J.; Fabian, A.C.; Roediger, E.; van Weeren, R.J.; Richard-Laferrière, A.; et al. VLA Resolves Unexpected Radio Structures in the Perseus Cluster of Galaxies. *Astrophys. J.* **2021**, *911*, 56. [CrossRef]
85. Enßlin, T.A.; Gopal-Krishna. Reviving fossil radio plasma in clusters of galaxies by adiabatic compression in environmental shock waves. *Astron. Astrophys.* **2001**, *366*, 26–34. [CrossRef]
86. Enßlin, T.A.; Brüggen, M. On the formation of cluster radio relics. *Mon. Not. R. Astron. Soc.* **2002**, *331*, 1011–1019. [CrossRef]
87. Markevitch, M.; Govoni, F.; Brunetti, G.; Jerius, D. Bow Shock and Radio Halo in the Merging Cluster A520. *Astrophys. J.* **2005**, *627*, 733–738. [CrossRef]
88. ZuHone, J.A.; Markevitch, M.; Lee, D. Sloshing of the Magnetized Cool Gas in the Cores of Galaxy Clusters. *Astrophys. J.* **2011**, *743*, 16. [CrossRef]
89. Botteon, A.; Gastaldello, F.; ZuHone, J.A.; Balboni, M.; Bartalucci, I.; Brunetti, G.; Bonafede, A.; Brüggen, M.; Shimwell, T.W.; van Weeren, R.J. A radio bubble shredded by gas sloshing? *Mon. Not. R. Astron. Soc.* **2024**, *527*, 919–930. [CrossRef]
90. Pacholczyk, A.; Scott, J. In situ particle acceleration and physical conditions in radio tail galaxies. *Astrophys. J.* **1976**, *203*, 313–322. [CrossRef]
91. Wilson, A.; Vallée, J.P. The structures of the head-tail radio galaxies IC 708 and IC 711 at 1.4 GHz. *Astron. Astrophys.* **1977**, *58*, 79–91.
92. Jones, T.W.; Owen, F.N. Hot gas in elliptical galaxies and the formation of head-tail radio sources. *Astrophys. J.* **1979**, *234*, 818–824. [CrossRef]

93. Brunetti, G.; Setti, G.; Feretti, L.; Giovannini, G. Particle reacceleration in the Coma cluster: Radio properties and hard X-ray emission. *Mon. Not. R. Astron. Soc.* **2001**, *320*, 365–378. [CrossRef]
94. Petrosian, V. On the Nonthermal Emission and Acceleration of Electrons in Coma and Other Clusters of Galaxies. *Astrophys. J.* **2001**, *557*, 560–572. [CrossRef]
95. Clarke, T.E.; Randall, S.W.; Sarazin, C.L.; Blanton, E.L.; Giacintucci, S. Chandra View of the Ultra-steep Spectrum Radio Source in A2443: Merger Shock-induced Compression of Fossil Radio Plasma? *Astrophys. J.* **2013**, *772*, 84. [CrossRef]
96. Ogrean, G.; Brüggen, M.; van Weeren, R.J.; Simionescu, A.; Röttgering, H.J.; Croston, J. Evidence for a merger-revived radio phoenix in MaxBCG J217.95869+13.53470. *Mon. Not. R. Astron. Soc.* **2011**, *414*, 1175–1182. [CrossRef]
97. Schellenberger, G.; Giacintucci, S.; Lovisari, L.; O'Sullivan, E.; Vrtilek, J.M.; David, L.P.; Melin, J.B.; Lal, D.V.; Ettori, S.; Kolokythas, K.; et al. The Unusually Weak and Exceptionally Steep Radio Relic in A2108. *Astrophys. J.* **2022**, *925*, 91. [CrossRef]
98. Rahaman, M.; Raja, R.; Datta, A.; Burns, J.O.; Rapetti, D. On the origin of diffuse radio emission in Abell 85-insights from new GMRT observations. *Mon. Not. R. Astron. Soc.* **2022**, *515*, 2245–2255. [CrossRef]
99. Whyley, A.; Randall, S.W.; Clarke, T.E.; van Weeren, R.J.; Rajpurohit, K.; Forman, W.R.; Edge, A.C.; Blanton, E.L.; Lovisari, L.; Intema, H.T. Understanding the Nature of the Ultra-Steep Spectrum Diffuse Radio Source in the Galaxy Cluster Abell 272. *arXiv* **2024**, arXiv:2402.04876.
100. Bonafede, A.; Intema, H.T.; Brüggen, M.; Girardi, M.; Nonino, M.; Kantharia, N.G.; van Weeren, R.J.; Röttgering, H.J. Evidence for Particle Re-acceleration in the Radio Relic in the Galaxy Cluster PLCKG287.0+32.9. *Astrophys. J.* **2014**, *785*, 1. [CrossRef]
101. Shimwell, T.W.; Markevitch, M.; Brown, S.; Feretti, L.; Gaensler, B.M.; Johnston-Hollitt, M.; Lage, C.; Srinivasan, R. Another shock for the Bullet cluster, and the source of seed electrons for radio relics. *Mon. Not. R. Astron. Soc.* **2015**, *449*, 1486–1494. [CrossRef]
102. Botteon, A.; Gastaldello, F.; Brunetti, G.; Dallacasa, D. A shock at the radio relic position in Abell 115. *Mon. Not. R. Astron. Soc.* **2016**, *460*, L84–L88. [CrossRef]
103. Di Gennaro, G.; van Weeren, R.J.; Hoeft, M.; Kang, H.; Ryu, D.; Rudnick, L.; Forman, W.R.; Röttgering, H.J.; Brüggen, M.; Dawson, W.A.; et al. Deep Very Large Array Observations of the Merging Cluster CIZA J2242.8+5301: Continuum and Spectral Imaging. *Astrophys. J.* **2018**, *865*, 24. [CrossRef]
104. Stuardi, C.; Bonafede, A.; Wittor, D.; Vazza, F.; Botteon, A.; Locatelli, N.; Dallacasa, D.; Golovich, N.R.; Hoeft, M.; van Weeren, R.J.; et al. Particle re-acceleration and Faraday-complex structures in the RXC J1314.4-2515 galaxy cluster. *Mon. Not. R. Astron. Soc.* **2019**, *489*, 3905–3926. [CrossRef]
105. Button, C.; Marchegiani, P. The application of the adiabatic compression scenario to the radio relic in the galaxy cluster Abell 3411–3412. *Mon. Not. R. Astron. Soc.* **2020**, *499*, 864–872. [CrossRef]
106. Velović, V.; Cotton, W.D.; Filipović, M.D.; Norris, R.P.; Barnes, L.A.; Condon, J.J. MeerKAT view of the dancing ghosts-peculiar galaxy pair PKS 2130-538 in Abell 3785. *Mon. Not. R. Astron. Soc.* **2023**, *523*, 1933–1945. [CrossRef]
107. Raja, R.; Rahaman, M.; Datta, A.; Smirnov, O.M. A radio bridge connecting the minihalo and phoenix in the Abell 85 cluster. *Mon. Not. R. Astron. Soc.* **2023**, *526*, L70–L76. [CrossRef]
108. Ramatsoku, M.; Murgia, M.; Vacca, V.; Serra, P.; Makhathini, S.; Govoni, F.; Smirnov, O.; Andati, L.A.L.; de Blok, E.; Józsa, G.I.G.; et al. Collimated synchrotron threads linking the radio lobes of ESO 137-006. *Astron. Astrophys.* **2020**, *636*, L1. [CrossRef]
109. Rudnick, L.; Cotton, W.; Knowles, K.; Kolokythas, K. One Source, Two Source(s): Ribs and Tethers. *Galaxies* **2021**, *9*, 81. [CrossRef]
110. Condon, J.J.; Cotton, W.; White, S.V.; Legodi, S.; Goedhart, S.; McAlpine, K.; Ratcliffe, S.; Camilo, F. Threads, Ribbons, and Rings in the Radio Galaxy IC 4296. *Astrophys. J.* **2021**, *917*, 18. [CrossRef]
111. Brienza, M.; Shimwell, T.W.; de Gasperin, F.; Bikmaev, I.; Bonafede, A.; Botteon, A.; Brüggen, M.; Brunetti, G.; Burenin, R.; Capetti, A.; et al. A snapshot of the oldest active galactic nuclei feedback phases. *Nat. Astron.* **2021**, *5*, 1261–1267. [CrossRef]
112. Rudnick, L.; Brüggen, M.; Brunetti, G.; Cotton, W.D.; Forman, W.; Jones, T.W.; Nolting, C.; Schellenberger, G.; van Weeren, R. Intracluster Magnetic Filaments and an Encounter with a Radio Jet. *Astrophys. J.* **2022**, *935*, 168. [CrossRef]
113. Jaffe, W.J. Origin and transport of electrons in the halo radio source in the Coma cluster. *Astrophys. J.* **1977**, *212*, 1–7. [CrossRef]
114. Venturi, T.; Bardelli, S.; Dallacasa, D.; Brunetti, G.; Giacintucci, S.; Hunstead, R.W.; Morganti, R. The radio halo in the merging cluster A3562. *Astron. Astrophys.* **2003**, *402*, 913–920. [CrossRef]
115. Brunetti, G.; Setti, G.; Comastri, A. Inverse Compton X-rays from strong FRII radio-galaxies. *Astron. Astrophys.* **1997**, *325*, 898–910. [CrossRef]
116. Blasi, P.; Colafrancesco, S. Cosmic rays, radio halos and nonthermal X-ray emission in clusters of galaxies. *Astropart. Phys.* **1999**, *122*, 169–183. [CrossRef]
117. Aleksić, J.; Antonelli, L.A.; Antoranz, P.; Backes, M.; Baixeras, C.; Balestra, S.; Barrio, J.A.; Bastieri, D.; Becerra González, J.; Bednarek, W.; et al. MAGIC Gamma-ray Telescope Observation of the Perseus Cluster of Galaxies: Implications for Cosmic Rays, Dark Matter, and NGC 1275. *Astrophys. J.* **2010**, *710*, 634–647. [CrossRef]
118. Ackermann, M.; Ajello, M.; Albert, A.; Allafort, A.; Atwood, W.B.; Baldini, L.; Ballet, J.; Barbiellini, G.; Bastieri, D.; Bechtol, K.; et al. Search for Cosmic-Ray-induced Gamma-Ray Emission in Galaxy Clusters. *Astrophys. J.* **2014**, *787*, 18. [CrossRef]
119. Ackermann, M.; Ajello, M.; Albert, A.; Atwood, W.; Baldini, L.; Ballet, J.; Barbiellini, G.; Bastieri, D.; Bechtol, K.; Bellazzini, R.; et al. Search for Gamma-Ray Emission from the Coma Cluster with Six Years of Fermi-LAT Data. *Astrophys. J.* **2016**, *819*, 149. [CrossRef]

120. Gupta, N.; Saro, A.; Mohr, J.J.; Benson, B.A.; Bocquet, S.; Capasso, R.; Carlstrom, J.E.; Chiu, I.; Crawford, T.M.; de Haan, T.; et al. High-frequency cluster radio galaxies: Luminosity functions and implications for SZE-selected cluster samples. *Mon. Not. R. Astron. Soc.* **2017**, *467*, 3737–3750. [CrossRef]
121. Böckmann, K.; Brüggen, M.; Koribalski, B.; Veronica, A.; Reiprich, T.H.; Bulbul, E.; Bahar, Y.E.; Balzer, F.; Comparat, J.; Garrel, C.; et al. Central radio galaxies in galaxy clusters: Joint surveys by eROSITA and ASKAP. *Astron. Astrophys.* **2023**, *677*, A188. [CrossRef]
122. Stimpson, M.; Hardcastle, M.J.; Krause, M.G.H. Numerical modelling of the lobes of radio galaxies-Paper V: Universal pressure profile cluster atmospheres. *Mon. Not. R. Astron. Soc.* **2023**, *526*, 3421–3440. [CrossRef]
123. Völk, H.J.; Atoyan, A.M. Clusters of galaxies: Magnetic fields and nonthermal emission. *Astropart. Phys.* **1999**, *11*, 73–82. [CrossRef]
124. Farber, R.; Ruszkowski, M.; Yang, H.Y.K.; Zweibel, E.G. Impact of Cosmic-Ray Transport on Galactic Winds. *Astrophys. J.* **2018**, *856*, 112. [CrossRef]
125. Brüggen, M.; Kaiser, C.R.; Churazov, E.; Enßlin, T.A. Simulation of radio plasma in clusters of galaxies. *Mon. Not. R. Astron. Soc.* **2002**, *331*, 545–555. [CrossRef]
126. Mendygral, P.J.; Jones, T.W.; Dolag, K. MHD Simulations of Active Galactic Nucleus Jets in a Dynamic Galaxy Cluster Medium. *Astrophys. J.* **2012**, *750*, 166. [CrossRef]
127. Turner, R.J.; Shabala, S.S. Dynamics of Powerful Radio Galaxies. *Galaxies* **2023**, *11*, 87. [CrossRef]
128. Yates-Jones, P.M.; Shabala, S.S.; Power, C.; Krause, M.G.H.; Hardcastle, M.J.; Mohd Noh Velastín, E.A.N.; Stewart, G.S.C. CosmoDRAGoN simulations—I. Dynamics and observable signatures of radio jets in cosmological environments. *Publ. Astron. Soc. Aust.* **2023**, *40*, e014. [CrossRef]
129. Shabala, S.; Yates-Jones, P.; Jerrim, L.; Turner, R.; Krause, M.; Norris, R.; Koribalski, B.; Filipovic, M.; Rudnick, L.; Power, C.; et al. Are Odd Radio Circles phoenixes of powerful radio galaxies? *arXiv* **2024**, arXiv:2402.09708.
130. Kang, H. Re-Acceleration of Fossil Electrons by Shocks Encountering Hot Bubbles in the Outskirts of Galaxy Clusters. *J. Korean Astron. Soc.* **2018**, *51*, 185–195. [CrossRef]
131. Kang, H.; Ryu, D. Curved Radio Spectra of Weak Cluster Shocks. *Astrophys. J.* **2015**, *809*, 186. [CrossRef]
132. Jones, T.W.; Nolting, C.; O'Neill, B.J.; Mendygral, P.J. Using collisions of AGN outflows with ICM shocks as dynamical probes. *Phys. Plasmas* **2017**, *24*, 041402. [CrossRef]
133. Nolting, C.; Jones, T.W.; O'Neill, B.J.; Mendygral, P. Interactions between Radio Galaxies and Cluster Shocks. I. Jet Axes Aligned with Shock Normals. *Astrophys. J.* **2019**, *876*, 154. [CrossRef]
134. Nolting, C.; Jones, T.W.; O'Neill, B.J.; Mendygral, P. Simulated Interactions between Radio Galaxies and Cluster Shocks. II. Jet Axes Orthogonal to Shock Normals. *Astrophys. J.* **2019**, *885*, 80. [CrossRef]
135. Nolting, C.; Ball, J.; Nguyen, T.M. Simulations of Precessing Jets and the Formation of X-shaped Radio Galaxies. *Astrophys. J.* **2023**, *948*, 25. [CrossRef]
136. ZuHone, J.; Ehlert, K.; Weinberger, R.; Pfrommer, C. Turning AGN Bubbles into Radio Relics with Sloshing: Modeling CR Transport with Realistic Physics. *Galaxies* **2021**, *9*, 91. [CrossRef]
137. Vazza, F.; Wittor, D.; Brunetti, G.; Brüggen, M. Simulating the transport of relativistic electrons and magnetic fields injected by radio galaxies in the intracluster medium. *Astron. Astrophys.* **2021**, *653*, A23. [CrossRef]
138. Vazza, F.; Wittor, D.; Di Federico, L.; Brüggen, M.; Brienza, M.; Brunetti, G.; Brighenti, F.; Pasini, T. Life cycle of cosmic-ray electrons in the intracluster medium. *Astron. Astrophys.* **2023**, *669*, A50. [CrossRef]
139. Vazza, F.; Wittor, D.; Brüggen, M.; Brunetti, G. Simulating the Enrichment of Fossil Radio Electrons by Multiple Radio Galaxies. *Galaxies* **2023**, *11*, 45. [CrossRef]
140. Inchingolo, G.; Wittor, D.; Rajpurohit, K.; Vazza, F. Radio relics radio emission from multishock scenario. *Mon. Not. R. Astron. Soc.* **2022**, *509*, 1160–1174. [CrossRef]
141. Smolinski, D.C.; Wittor, D.; Vazza, F.; Brüggen, M. A multishock scenario for the formation of radio relics. *Mon. Not. R. Astron. Soc.* **2023**, *526*, 4234–4244. [CrossRef]
142. Vazza, F.; Brüggen, M.; van Weeren, R.; Bonafede, A.; Dolag, K.; Brunetti, G. Why are central radio relics so rare? *Mon. Not. R. Astron. Soc.* **2012**, *421*, 1868–1873. [CrossRef]
143. Nuza, S.E.; Gelszinnis, J.; Hoeft, M.; Yepes, G. Can cluster merger shocks reproduce the luminosity and shape distribution of radio relics? *Mon. Not. R. Astron. Soc.* **2017**, *470*, 240–263. [CrossRef]
144. Hitomi Collaboration. The quiescent intracluster medium in the core of the Perseus cluster. *Nature* **2016**, *535*, 117–121. [CrossRef] [PubMed]